ADVANCED FUNCTIONAL MATERIALS
www.afm-journal.de

The Effect of Ageing on Exciton Dynamics, Charge Separation, and Recombination in P3HT/PCBM Photovoltaic Blends

Felix Deschler, Antonietta De Sio, Elizabeth von Hauff, Peter Kutka, Tobias Sauermann, Hans-J. Egelhaaf, Jens Hauch, and Enrico Da Como**

A study of how light-induced degradation influences the fundamental photophysical processes in the active layer of poly(3-hexylthiophene)/[6,6]-phenyl C_{61}-butyric acid methyl ester (P3HT/PCBM) solar cells is presented. Non-encapsulated samples are systematically aged by exposure to AM 1.5 illumination in the presence of dry air for different periods of time. The extent of degradation is quantified by the relative loss in the absorption maximum of the P3HT, which is varied in the range 0% to 20%. For degraded samples an increasing loss in the number of excitons within the P3HT domains is observed with longer ageing periods. This loss occurs rapidly, within the first 15 ps after photoexcitation. A more pronounced decrease in the population of polarons than excitons is observed, which also occurs on a timescale of a few picoseconds. These observations, complemented by a quantitative analysis of the polaron and exciton population dynamics, unravel two primary loss mechanisms for the performances of aged P3HT/PCBM solar cells. One is an initial ultrafast decrease in the polaron generation, apparently not related to the exciton diffusion to the polymer/fullerene interface; the second, less significant, is a loss in the exciton population within the photoexcited P3HT domains. The steady-state photoinduced absorption spectra of degraded samples exhibits the appearance of a signal ascribed to triplet excitons, which is absent for non-degraded samples. This latter observation is interpreted considering the formation of degraded sites where intersystem crossing and triplet exciton formation is more effective. The photovoltaic characteristics of same blends are also studied and discussed by comparing the decrease in the overall power conversion efficiency of solar cells.

1. Introduction

Organic solar cells continue to attract a large interest because of their potential for simple processing methods, lightweight applications, and low production costs.[1] During recent years there has been a huge improvement in the power conversion efficiencies of both single-junction and tandem-cell devices.[2,3] Recent reports show photovoltaic efficiencies reaching 8% by a combination of low bandgap donor–acceptor copolymers and a fullerene derivative.[2,4] A topic which has only been marginally investigated, but which is just as important for commercialization, is long-term device stability. Indeed, estimations on the costs of production and cells lifetime indicate that organic photovoltaics can become competitive with other technologies if module lifetimes of 5 to 10 years can be attained.[1,5] Studies on the long-term stability and the degradation of solar cells have thus far been mainly focussed on complete devices.[6–11] While those are of primary importance, it is not always possible to distinguish between degradation of the active layer, the interface with the electrodes, or the contacts.[12,13] For example, in devices with regular structure the corrosion of the low workfunction electrodes usually limits the lifetime.[10] We have recently shown that in cells with inverted structure the degradation under illumination in dry air affects mainly the active layer, consisting of a reversible part which is assigned to oxygen-induced doping and an irreversible part which is due to photo-oxidation.[14] In principle, the elegant combination of photoluminescence (PL) and electroluminescence imaging can

F. Deschler, Dr. E. Da Como
Photonics and Optoelectronics Group
Department of Physics and CeNS
Ludwig-Maximilians-Universität
80799, Munich, Germany
E-mail: enrico.dacomo@physik.uni-muenchen.de

A. De Sio
Institute of Physics
Energy and Semiconductor Research Laboratory Carl von Ossietzky University
26111 Oldenburg, Germany

Prof. E. von Hauff
Fraunhofer Institute for Solar Energy Systems (ISE)
Freiburg, Germany
Albert-Ludwigs-Universität Freiburg
Physikalisches Institut
79104, Freiburg, Germany
E-mail: elizabeth.v.hauff@physik.uni-freiburg.de

P. Kutka, T. Sauermann, Dr. H.-J. Egelhaaf, Dr. J. Hauch
Konarka Technologies GmbH
90443 Nürnberg, Germany

DOI: 10.1002/adfm.201101923

distinguish between degradation of the active layer or electrodes in a complete device.[15] However, considering the active layer per se, it is already a formidable task to unravel and pinpoint the physical processes responsible for photovoltaic action, each of which might be undesirably influenced by degradation. In a recent systematic work Reese et al. studied the photodegradation of the active layer and quantified the changes in photoconductance by time resolved microwave conductivity.[16] Such a technique offers the advantage of measuring the photocurrent in the blend without the complications of extracting charges with electrodes; on the other hand, it can overlook the dynamics of the initial photoexcitations, because of poor time resolution in the nanosecond regime. In addition, the experiment remains essentially sensitive only to the photocarriers.[17]

Indeed, there are a number of different physical processes contributing to photocurrent in a typical polymer/fullerene solar cell. First, upon light absorption electron–hole pairs are created. This process takes place primarily in the conjugated polymer, because of the high absorption cross-section of optical transitions which are instead forbidden and thus weak for most fullerene derivatives.[18–20] A large number of electron–hole pairs form excitons, which undergo diffusion and recombination, the rest are expected to form polaron pairs.[21,22] Before recombining, the vast majority of excitons reaches the heterojunction where electron transfer occurs, provided that an optimal bulk heterojunction morphology is present.[23–25] Polaron pairs at the heterojunction can separate to form free carriers or recombine via interfacial charge-transfer excitons.[26–29] Separated positive and negative carriers (polarons) then move towards the electrodes within the polymer and fullerene domains, respectively. The photocurrent is the result of polaron drift and extraction at the electrodes. From previous studies, it has not been established which is the contribution of each process and species in limiting the performances of aged devices; in other words, whether excitons, polarons or the charge transfer states are mainly affected by ageing and to what extent. The degradation of the polymer/fullerene active layer occurring upon extended illumination in the atmosphere can in principle impact each physical process described above. For example, exciton recombination via dark states could be accelerated, negatively influencing the total amount of polaron pairs supposed to be generated at the heterojunction. Also polarons might be trapped and their recombination rate increased because of the loss in the average carrier mobility, which is known to accelerate recombination.[30,31]

In this paper, we address the role of irreversible degradation on the fundamental steps in photovoltaic action for the model system regioregular poly(3-hexylthiophene)/[6,6]-phenyl C_{61}-butyric acid methyl ester (P3HT/PCBM) blends. We used time-resolved photoinduced absorption (PIA) spectroscopy to gain valuable insights on the population dynamics of excitons and polarons for different levels of ageing. We show that degradation has an influence on both the exciton and polaron populations. Within the first 15 ps after optical excitation, during which time period exciton diffusion to the heterojunction is expected to occur and polarons are created, we observe a difference in the relative loss of these two species. In general, for all studied samples the loss in polarons is larger than the one in excitons. By using steady-state PIA spectroscopy we show that the loss in singlet excitons results in the appearance of a long-lived population of triplets. We provide a complete overview of how ageing, by exposure to light, influences the photophysics of P3HT/PCBM blends and quantify the loss mechanisms by means of a coupled rate equation model. The paper is structured in the following way: first the loss in absorption of the active layer is quantified by linear absorption spectroscopy. This is used to evaluate the degree of degradation and classify the different samples studied. The influence of degradation on the exciton and polaron relative populations is studied by steady-state photoluminescence (PL) and PIA spectroscopy. The differences in the population dynamics are then rationalized using time-resolved PL and PIA spanning the time range from hundreds of femtoseconds (fs) to around 1 nanosecond (ns). In addition, we report solar cells prepared with degraded blends and discuss the implications of our findings for real devices.

2. Results

2.1. Exciton Creation and Recombination

Figure 1a shows the absorption spectra of four P3HT/PCBM (1:0.8 weight) blends differing in the time of exposure to an AM1.5 solar simulator in dry air and at room temperature. All the spectra show the typical absorption features of annealed P3HT/PCBM blends in the visible and UV.[32] The absorption in the visible is mainly due to the conjugated polymer, since PCBM has only a weak absorption tail extending into this region.[18] While the P3HT absorption band is monotonically decreasing with exposure time (see inset), the absorption of PCBM, which is more pronounced in the UV below 350 nm, is less affected. This observation suggests that PCBM is less likely influenced by the degradation recipe followed here and probably more robust than P3HT. Remarkably, the decrease in the absorption spectrum of P3HT seems to be wavelength independent (all spectra have similar shapes) and only a very weak feature on the red onset of the absorption is noticed after relative subtraction of the spectra (not shown). Following the results of Reese et al.,[16] the short exposure times (ageing time periods) used in our study exclude changes to the initial morphology after preparation of the blends.

In Figure 1b we report the ratio of the integrated P3HT PL (wavelength integration interval 550 to 950 nm) of the non-degraded blend, PL(0%), to those for the degraded samples, PL (x%), where x indicates the level of ageing as illustrated in Figure 1a. The integrated PL is evaluated after rescaling for the number of photons absorbed at the exciting wavelength of 500 nm. The data points indicate a hyperbolic behaviour, typical of a Stern-Volmer type quenching.[33] The Stern-Volmer behavior suggests that excitons diffusing in the polymer domains encounter quenching sites, whose density increases approximately linearly with the observed absorbance loss. Therefore, blend films exposed for longer time intervals to illumination have a higher concentration of quenching sites, likely related to species generated during

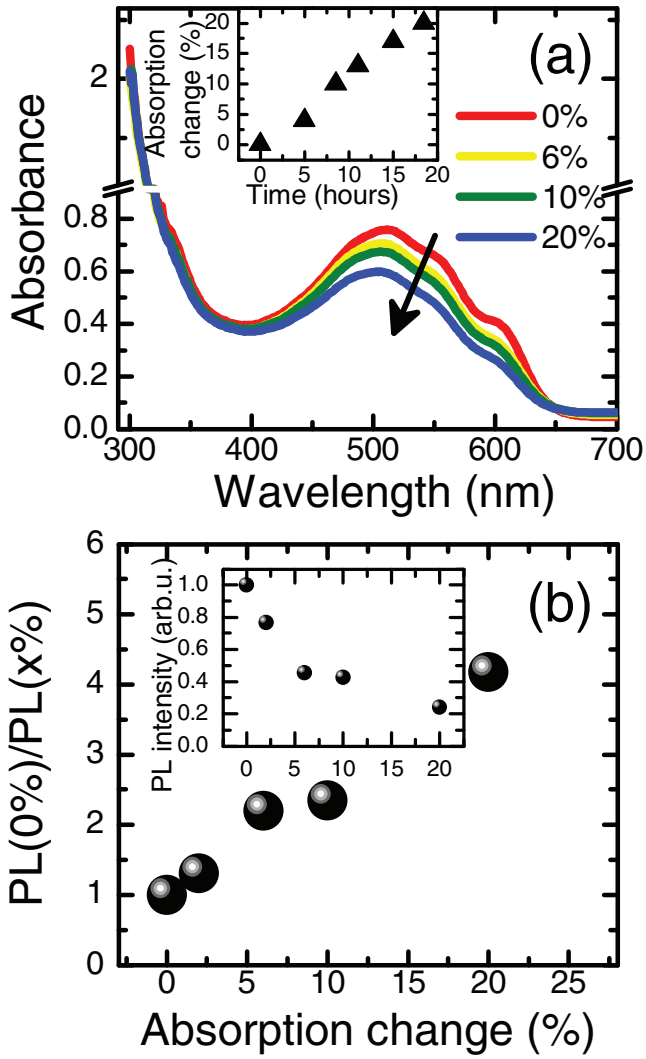

Figure 1. a) Absorption spectra of P3HT/PCBM blends subjected to different ageing periods of illumination in dry synthetic air. The relative loss in% of the absorption at 500 nm is used to classify the samples where 0% corresponds to the non-degraded sample. The inset shows the absorption change as a function of the illumination time in hours. b) Ratio between the integrated PL between 550 and 950 nm of the non-degraded sample [PL(0%)] and degraded sample [PL(*x*%)] as a function of the change in absorption due to degradation as illustrated in (a). The inset shows the integrated PL of each sample as a function of the absorption change on a normalized intensity scale.

the photo-oxidation process. Those species appear to be dark, since we were unable to detect significant differences in the shape of the PL spectra in the visible and near infrared up to 1400 nm (not shown). Summarizing the information extracted from the PL experiments is that photogenerated excitons in P3HT can decay non-radiatively as a consequence of interaction with dark species, produced in the degradation process. Some excitons might be also quenched by charges, originating from radical-like reactions during degradation.[34] For excitons in P3HT this is expected to be a loss channel competing with diffusion to the heterojunction interface and charge separation.

2.2. Polaron and Exciton Population Dynamics

The PL data of Figure 1 provide valuable information on the quenching of excitons after degradation, but do not offer a probe for the charge-transfer process, which takes place at the interface with PCBM and results in the formation of polarons, i.e., the free carriers responsible for photocurrent. An experimental technique which gives unique insights into the population dynamics of both excitons and polarons is PIA spectroscopy. We first comment on the different signals obtained in such experiments in steady-state conditions and then focus our attention on the dynamics in the picosecond timescale.

Figure 2 shows the continuous wave (cw)-PIA of the samples at different degradation stages. In PIA the relative differential transmission, $\Delta T/T$, of light from a lamp passing through the blend film is measured with and without laser excitation, which is centred at 532 nm for the experiment shown. Negative signals in the graphs reported in this paper (note the $-\Delta T/T$ in the vertical scale) indicate an increase in the transmitted probe light and can originate from ground-state bleaching (GBS) or stimulated emission (SE). Positive signals are due to a decrease in the transmitted light and originate from exciton absorption towards higher excited states or from polaron absorption. The cw-PIA spectrum of P3HT/PCBM is dominated by the optical transition of species in P3HT, which have been previously studied and interpreted.[35] In Figure 2 the band at 670 nm has been assigned to delocalized polarons (DP), meaning polarons delocalized over two or more polymeric chains, while the weak signal above 1100 nm is due to absorption transitions from the first excitonic state (S_1) to a higher exciton states (S_n).[35,36] We denote this exciton absorption (ExA) and it is expected to

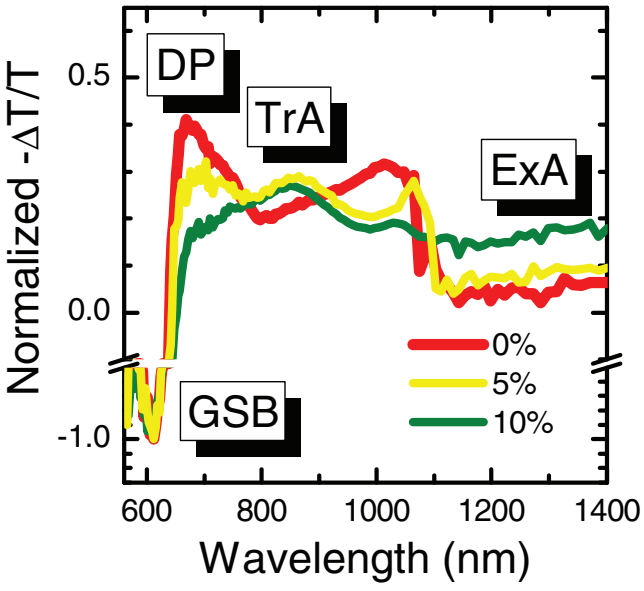

Figure 2. cw-PIA of P3HT/PCBM blends at 0%, 5% and 10% degradation. The different transitions are indicated as ground-state bleaching (GSB), delocalized polarons (DP), triplet exciton absorption (TrA) and singlet exciton absorption (ExA). Excitation was performed at 532 nm. The spectra were normalized for the GSB which monitors the overall amount of excited species in the blend. Note the break in the $\Delta T/T$ vertical scale.

be weak in a steady-state experiment because of the short lived nature of excitons in a polymer fullerene blend.[21] Peaks at 850 nm are due to triplet exciton absorption ($T_1 \rightarrow T_n$) and at 1050 nm to polarons with intrachain character.[37] Upon ageing we note that there is a monotonic decrease in the amplitude of the DP signal, indicating that degradation has an influence on the population of polarons. While the 0% sample (red curve) has only two prominent bands at 670 nm (DP) and around 1000 nm due to polarons, the 5% and 10% samples exhibit a signal at 850 nm, which we interpret as being due to triplet exciton absorption (TrA). This excited state transition is usually not observed in regioregular P3HT in blends with PCBM, since the relatively high yield of polaron formation in the excited state competes with intersystem crossing of singlet excitons and population of the triplet state.[22] Supporting this, PIA investigations on regiorandom P3HT, where polymer chains are more disordered and polaron generation is less probable,[27,38] show the presence of a band at 850 nm with spin-1 characteristics, i.e., a triplet.[35,39] In contrast, we note little change in the ExA spectral range among the different samples. Because of the short lived nature of singlet excitons in P3HT/PCBM those are almost undetectable in steady-state experiments, like the one shown in Figure 2. We prefer to address this point in a more quantitative manner below, by analyzing the transients on a picosecond timescale where excitons are apparent.

In order to probe the exciton dynamics we performed fs-PIA spectroscopy by exciting the sample with 200 fs pulses centred at 550 nm and recording the change in transmission of time delayed pulses at 1500 nm. This probe wavelength allows us to observe the rise and decay of ExA, in a spectral region well separated from the contribution of polarons.[38] Here, we have removed a small long-living background, likely caused by a weak polaron signal from PCBM, since its anion is expected to absorb in this region.[40] **Figure 3**a shows the $\Delta T/T$ transients probing the ExA for the different blends, rescaled for the number of absorbed photons. For all samples the signal sets in within our time resolution of approximately 250 fs, but shows different amplitudes at zero time delay and a faster initial decay in the degraded samples as compared to the non-degraded blend (0%, red curve). This clearly indicates that in the degraded samples part of the initial hot excitons do not contribute to this signal within the first 250 fs. By looking at the decay, when excitons are already thermalized, we note that degradation leads to a faster dynamic, suggesting that exciton quenching during the diffusion process of the first picoseconds contributes to the loss in the overall exciton population as well. It is interesting to

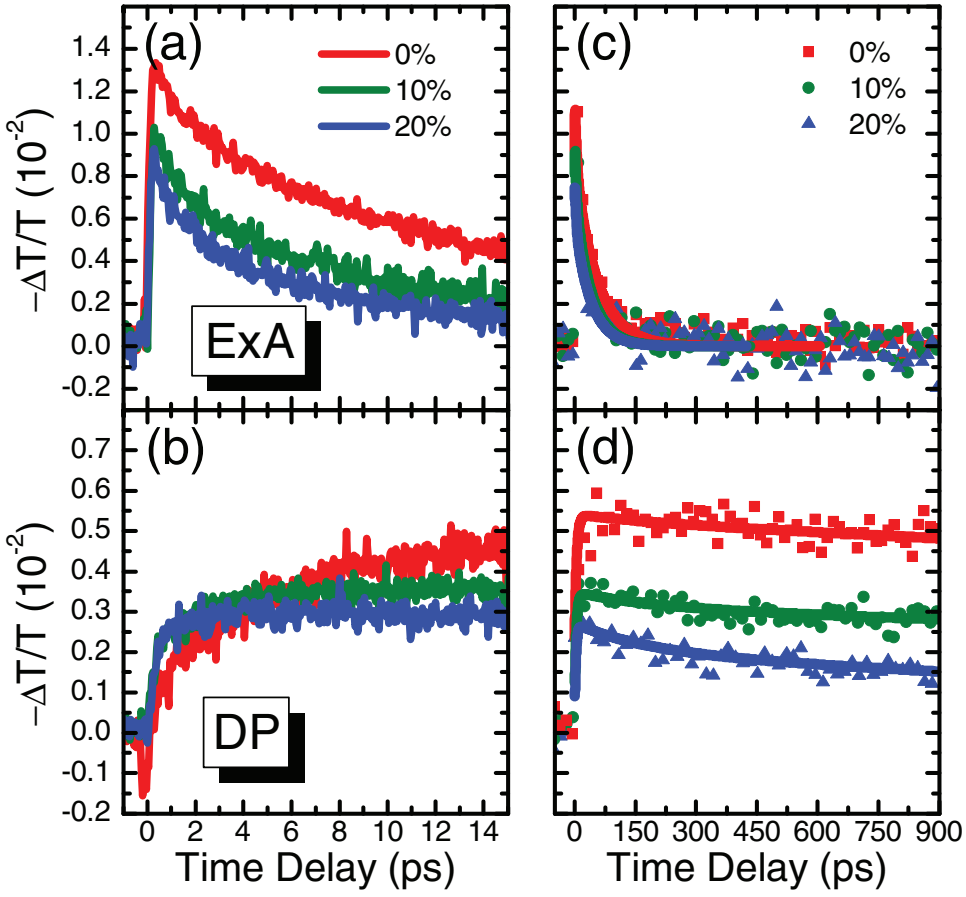

Figure 3. PIA transients for P3HT/PCBM blends with the probe centred in the absorption bands of excited singlet state (ExA, 1500 nm) and delocalized polaron (DP, 700 nm), respectively. a,b) Transient rises and decays on a short timescale (0–15 ps). c,d) transient decays on a long timescale (0–900 ps) for ExA and DP, respectively; symbols are data points whereas the solid lines represent fits according to the model of rate equations described in the text. Excitation performed at 550 nm with <10 μJ cm^{-2}. The transients have been rescaled for the amount of photons absorbed, i.e., 1–10$^{(-OD)}$ of the degraded samples at the exciting wavelength of 550 nm.

compare these decays with the dynamics of the DPs, which are supposed to be representative for the carriers contributing to photocurrent in the solar cell.[38]

In Figure 3b we report the transient dynamics of DPs probed at 700 nm. The non-degraded sample (red curve) at zero time delay shows an ultrafast negative feature (positive on a $+\Delta T/T$ scale) slightly longer than the duration of the pump-probe pulses, which evolves into a positive signal with a rather long *rise* time, reaching a maximum at approximately 40 ps. In the degraded samples the rise in DPs appears to be faster and the initial negative feature is absent. Another feature characterising degraded samples is that the overall amount of DP is smaller as the signals saturate at $-\Delta T/T = 0.52 \times 10^{-2}$ for the 0% sample, and 0.35×10^{-2} and 0.29×10^{-2} for the 10% and 20% samples, respectively. The rise appears to correspond to the decay of excitons seen in Figure 3a and it has been previously interpreted as the feeding of the free polarons from excitons or charge transfer excitons.[41,42] In contrast to these previous reports, we propose that the generation of DPs is not subjected to a rise, but rather the $\Delta T/T$ signal in this spectral region is superimposed to a short-lived SE feature.[21] The SE has dynamics resembling those of ExA (Figure 3a), since it originates from the same species, i.e., excitons in the P3HT domains, though they are not exactly identical. The reason is that SE is due to excitons recombining in the P3HT domains, whereas ExA in principle should originate from all the excitons photogenerated in P3HT, i.e., those recombining, trapping, or separating to form polarons at the heterojunction. To support the interpretation that the negative feature is due to SE, it is worthwhile noting that the loss of excitons at time zero seen in the ExA transients is reflected in the absence of the negative SE signal for the 10% and 20% samples in Figure 3b. If the rise in DP were due to the splitting of excitons after diffusion to the polymer/fullerene interface, the faster decay of ExA would mean a faster – thus more efficient – exciton separation towards carriers, which is not observed since the maximum DP amplitude decreases. For the 20% sample the rise of the DP signal appears to be instantaneous and uncorrelated to a diffusion of excitons towards the interface taking place within a few picoseconds. This interpretation is in agreement with recent experimental studies by infrared femtosecond PIA spectroscopy, where polarons can be selectively probed in the absence of superimposed stimulated emission contributions and appears without any rise on a picosecond timescale.[21,43] Further indication of the fact that in P3HT/PCBM blends a substantial amount of polarons is generated immediately after excitation and not as a consequence of exciton diffusion to the interface, is the different relative loss in excitons and DPs. For the 20% sample the initial loss in excitons with respect to the 0% sample, estimated at zero time delay is about 31%, whereas the loss in DPs, obtained from their maximum $\Delta T/T$, amounts to about 45%.

We have also studied the long timescale dynamics of these two photoexcitations, which are reported in Figure 3c and d for ExA and DP, respectively. While excitons are short-lived, the DPs show rather slow recombination dynamics. For the non-degraded sample, the transient, shown in red, does not exhibit a decay on a timescale of 1 ns in accordance with previous studies on non-degraded P3HT/PCBM blends.[21,38] This is consistent with the long-lived nature of the DPs, which are supposed to be extracted from the active layer and contribute to the photocurrent. In contrast, the 10% and 20% degraded samples exhibit an initial decay on the hundreds of picoseconds timescale. This confirms that the products resulting from photo-oxidation are also influencing the polaron dynamics at later times and evidently lead to an accelerated recombination. Summarizing, we stress that relative losses in exciton and polaron populations are not identical upon ageing of the blend. The loss in polarons seems to be more severe.

In order to obtain a quantitative estimation of the trapping rates involved in the loss process we have modelled the transient absorption curves with a system of coupled rate equations outlined here. First, we have considered that the initial hot excitons, [HEx], are branching into four different populations, which are the recombining excitons [Exr], the diffusing excitons [Exd], the free polarons [Polf] and trapped excitons [Ext] according to the rate equation:

$$\frac{d[\mathrm{HEx}]}{dt} = -\frac{[\mathrm{HEx}]}{\tau_{\mathrm{HEx-Polf}}} - \frac{[\mathrm{HEx}]}{\tau_{\mathrm{HEx-Exd}}} - \frac{[\mathrm{HEx}]}{\tau_{\mathrm{HEx-Exr}}} - \frac{[\mathrm{HEx}]}{\tau_{\mathrm{HEx-Ext}}} \quad (1)$$

This initial ultrafast partition or branching of HEx is a necessary step to describe the decrease in the signal of ExA and DP at zero time delay and consistent with the experimental reports that diffusing excitons are not the exclusive reservoir of polarons in P3HT/PCBM blends and the latter can form quasi-instantaneously.[21,43] Equation 1 takes into consideration the fact that a portion of the initial HEx is generated in P3HT close enough to the heterojunction interface to diffuse and reach PCBM, those constitute the diffusing excitons, Exd, while some other within the P3HT domains far from the interface are just recombining, Exr, or are trapped to dark states because of degradation products, Ext. The first term on the right hand side of Equation 1 takes into account the direct formation of polarons from the HEx as evidenced from the experiments by Piris et al.[21]

The time constants, or inverse probabilities, for the generation of free polarons $\tau_{\mathrm{HEx-Polf}}$, diffusing excitons $\tau_{\mathrm{HEx-Exd}}$, recombining and trapped excitons $\tau_{\mathrm{HEx-Exr}}$ and $\tau_{\mathrm{HEx-Ext}}$, respectively, determine the initial branching ratios in Equation 1. We have described the transient signal of ExA considering two contributions, one originating from diffusing excitons:

$$\frac{d[\mathrm{Exd}]}{dt} = \frac{[\mathrm{HEx}]}{\tau_{\mathrm{HEx-Exd}}} - \frac{[\mathrm{Exd}]}{\tau_{\mathrm{Diff}}} - \frac{[\mathrm{Exd}]}{\tau_{\mathrm{Exd-Polf}}} \quad (2)$$

and a second from recombining excitons:

$$\frac{d[\mathrm{Exr}]}{dt} = \frac{[\mathrm{HEx}]}{\tau_{\mathrm{HEx-Exr}}} - \frac{[\mathrm{Exr}]}{\tau_{\mathrm{Exr}}} \quad (3)$$

Both populations are fed by [HEx], i.e., the initial amount of hot excitons induced by the pump laser pulse, with the respective probabilities set by $\tau_{\mathrm{HEx-Exd}}$ and $\tau_{\mathrm{HEx-Exr}}$. These excitons are influenced by diffusion to the interface, τ_{Diff}, or formation of a trapped polaron, $\tau_{\mathrm{HEx-Polt}}$ in the case of Equation 2 and recombination τ_{Exr} for Equation 3. To model the transient DP absorption signal, we used two contributions originating from free and trapped polarons, [Polf] and [Polt], which are described by

ADVANCED FUNCTIONAL MATERIALS
www.afm-journal.de

Materials Views
www.MaterialsViews.com

$$\frac{d[\text{Polf}]}{dt} = \frac{[\text{Exd}]}{\tau_{\text{Diff}}} + \frac{[\text{HEx}]}{\tau_{\text{HEx}-\text{Polf}}} - \frac{[\text{Polf}]}{\tau_{\text{Polfr}}} \quad (4)$$

$$\frac{d[\text{Polt}]}{dt} = \frac{[\text{Exd}]}{\tau_{\text{Exd}-\text{Polt}}} - \frac{[\text{Polt}]}{\tau_{\text{Poltr}}} \quad (5)$$

The modelling with two polaron populations was necessary to consider the biexponential decay of Figure 3d for the degraded samples. In Equation 1 we optimized $\tau_{\text{HEx–Exd}}$ = 300 fs and $\tau_{\text{HEx–Exr}}$ = 100 fs for the non-degraded sample and kept them constant in the fitting of all the other curves. These lifetimes are in very good agreement with the typical thermalization rates of excitons measured in conjugated polymers.[44] The rates of free polaron formation $(\tau_{\text{HEx–Polf}})^{-1}$ and trapping of the hot excitons $(\tau_{\text{HEx–Ext}})^{-1}$, were varied because of degradation induced phenomena. In Equation 2 and 4 we kept constant τ_{Diff} = 6 ps and the rate of trapped polaron recombination τ_{Poltr} = 175 ps. Since this latter recombination rate does not involve mobile polarons but rather trapped we do not expect to have a substantial dependence on the level of ageing. τ_{Exr} was obtained from time resolved PL experiments (not shown). The six decay curves were then fitted adjusting the remaining four decay times and are shown as solid curves in Figure 3c,d. The fittings describe well the transient curves for all samples both in amplitude and dynamics.

We first discuss here the rates which were varied in order to obtain a decrease in the amplitude of both ExA and DP signals, during the time duration of the laser pulse. We notice that $1/\tau_{\text{HEx–Ext}}$, which is the rate at which hot excitons turn into trapped excitons, is an important fitting parameter in our model. For instance at 0% this rate can be as small as $(10\ \text{ps})^{-1}$, since the other more probable processes of Equation 1 dominate, while for increasing degradation levels it has to be set to a higher value of $(100\ \text{fs})^{-1}$ (see **Table 1**, second column). The initial decrease in DP signal could be described considering changes in $\tau_{\text{HEx-Polf}}$, which has a lower probability $(600\ \text{fs})^{-1}$ upon degradation, with respect to the 0% sample $(300\ \text{fs})^{-1}$. These two fitting parameters have an accuracy of about ±10 fs. For the different decays, the faster dynamics of ExA on a ps timescale upon degradation is described by decreasing $\tau_{\text{Exd-Polt}}$. This lifetime is also responsible for generating the correct amount of trapped polarons to fit the DP curves. Our model is also capable of reproducing the long decay time of DP, which appears to be dominated by two lifetimes. Here, we have decreased the recombination time of free polarons, τ_{Polfr}, from >10 ns in the 0% to 8 ns and 3 ns for the 10% and 20% samples, respectively (last column in Table 1). This recombination rate increases with ageing of samples and is consistent with a large number of defect sites induced by the degradation process. The first contribution in these curves is from the recombination of trapped polarons fixed at 175 ps.

Table 1. Time constant for the different photophysical processes described in Equation 1–5 considering samples showing 0%, 10% and 20% absorption loss.

Sample	$\tau_{\text{HEx–Ext}}$ [fs]	$\tau_{\text{Exd–Polt}}$ [ps]	$\tau_{\text{HEx - Polf}}$ [fs]	τ_{Polfr} [ns]
0%	10×10^3	100	300	10
10%	200	30	500	8
20%	100	10	600	3

Summarizing, the main message we can extract from the rate equation model is that the ultrafast initial loss in ExA and DP are due to an increased probability of trapping of hot excitons and a decreased probability of free polaron formation, respectively. These two trends are summarized in the second and fourth columns of Table 1 and determine the major initial losses. The faster decays observed in Figure 3a for the ExA upon degradation are due to the generation of trapped polarons by the diffusing excitons. Finally, the faster decay in the DP signal, which is observed in Figure 3d upon degradation, is a consequence of an increased population of trapped polarons and polaron recombination which enters the few nanosecond regime, last column of Table 1. **Figure 4** is a scheme summarizing the main photophysical processes in aged blends where the different mechanisms of trapping and recombination refer to Table 1.

While the initial ultrafast processes account for the major initial loss in the species contributing to the functioning of a solar

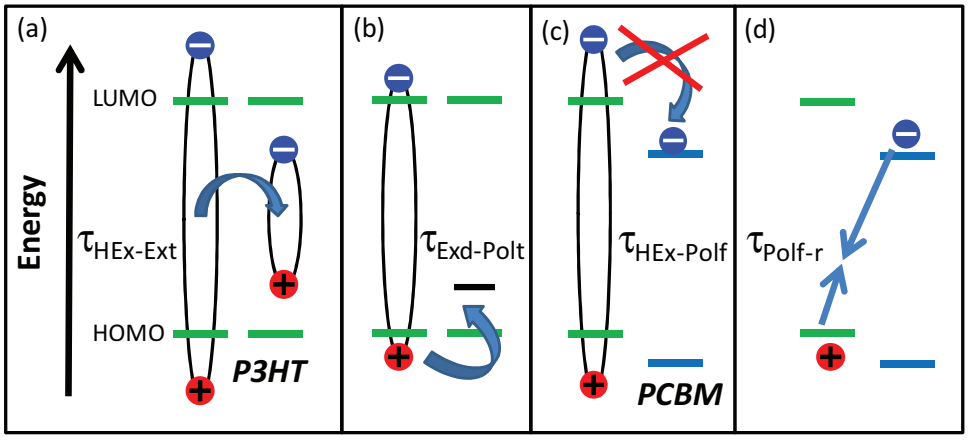

Figure 4. Energy scheme illustrating the different processes occurring in aged P3HT/PCBM blends, the highest occupied molecular orbital (HOMO) and lowest unoccupied molecular orbital (LUMO) of P3HT (green) and of PCBM (blue) are indicated on a vertical energy scale: a) hot exciton trapping in P3HT, b) exciton splitting by degradation products to form trapped polarons, c) hindered charge transfer at the interface between P3HT and PCBM, and, d) recombination of free polarons in P3HT. The processes illustrated here correspond to the lifetime presented in Table 1.

cell, the long timescale of DP recombination is seriously compromised for extensive degradation treatments, such as those used to obtain the 10% and 20% sample. Here, the long-lived polarons, which are contributing to the photocurrent, recombine in 8 and 3 ns, a lifetime that is prohibitive to reach efficient charge extraction, which usually occurs on a microsecond timescale.[45] To verify this prediction, we produced solar cells with the same materials following an identical ageing procedure and studied the current voltage characteristics upon illumination with a solar simulator.

2.3. Device Performance

In order to quantify the effect of degradation on device performance, P3HT:PCBM cells with inverted structure were characterized electrically after the degradation procedure. Devices with the stack ITO/hole-blocking-layer(HBL)/P3HT:PCBM were degraded for different periods of time in dry oxygen under illumination and the progress of degradation was monitored by UV/vis absorption. Degraded stacks, as well as non-degraded (kept in glovebox in dark during fabrication) were then completed by applying the PEDOT:PSS layer and the silver electrode (**Figure 5**a). Figure 5b shows the current voltage characteristics of two exemplary cells, degraded 0%, 2%, and 5%. An absorption loss of the active layer by 5% results in the reduction of device power conversion efficiency from $\eta = 2.9\%$ to about 0.23%. This loss is mainly due to a decrease in the short circuit current, from 8.1 to 1.0 mA cm^{-2}. The loss in fill factor is less dramatic from $FF = 0.64$ to 0.4 and, interestingly, we note that the open circuit voltage is not affected by degradation, at least up to 5%. The 88% loss in J_{sc} for a device with 5% absorption loss is a combination of several factors, about 24% are due to the reduction of charge-carrier formation (polarons) during the first 250 fs after the light pulse, as determined from the DP transient PIA signal (not shown). We conclude that the remaining 64% of loss in extracted charge carriers is due to loss in absorption (5%) and enhanced charge-carrier recombination on the microsecond timescale not accessible in the present experiments, or trapping in PCBM which is not evident in our data. Longer ageing periods corresponding to the 10% sample resulted in the total absence of photovoltaic response in the cells.

3. Discussion

The analysis of our photophysical data pinpoints the processes responsible for the degradation of performances in the active layer of polymeric solar cells based on P3HT/PCBM. In particular, the data presented in Figure 3 together with the rate equation model identify a faster trapping of the initial hot excitons and a less probable formation of free polarons during exciton relaxation. The experimental observation that the major losses are occurring while excitons have not yet completely relaxed indicates that hot excitons are more prone to undergo a trapping process with a degradation product or other processes diminishing their density. This hypothesis can be rationalized considering that hot excitons are more delocalized and in a coherent state. In this configuration they can experience a larger number of conjugated segments in the first few hundred femtoseconds and find a degradation product easily.[46]

The more significant loss in polarons which results in the decrease of the maximum amplitude reached by the DP absorption signal is a consequence of less probable free polaron formation and competing hot exciton trapping. In non-degraded systems such polarons are formed on an ultrafast timescale (<100 fs), involving those P3HT chromophores which are very close to the heterojunction interface. It is interesting that degradation of the polymer domains, which is demonstrated by our absorption and PL experiments (Figure 1), is influencing an ultrafast process occurring primarily for chromophores close to the interface. We suggest here that the degradation products, likely originating from photo-oxidation of the polymer, might be more concentrated at the heterojunction, where P3HT chains are at the border of a semi-crystalline domain and oxygen can diffuse easily with respect to the core of the domains.

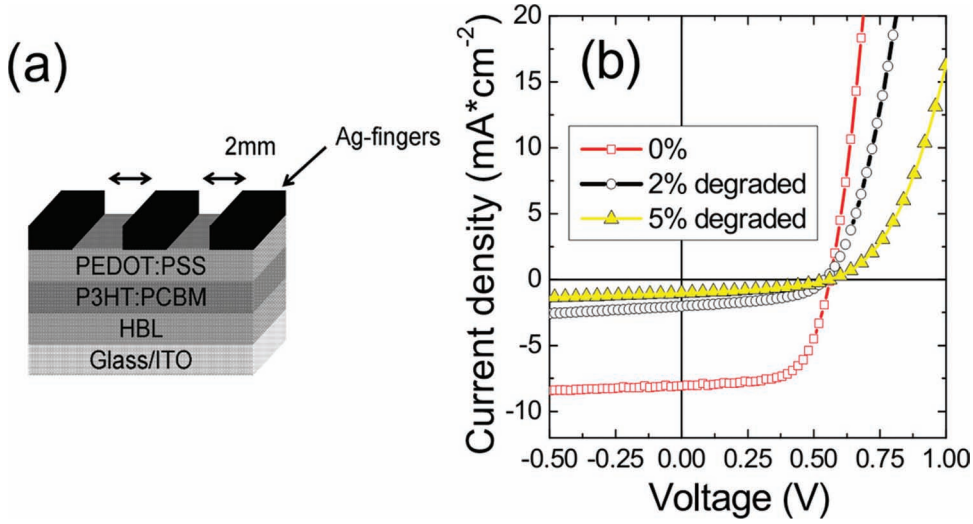

Figure 5. a) Structure of the solar cell used in the electrical measurements. b) Current density vs. bias voltage for a P3HT:PCBM device with inverted structure under illumination with a solar simulator before (red squares) and after (yellow triangles and black circles) degradation by illumination in dry synthetic air. The extent of degradation corresponds to an absorption loss of the active layer by 2% (black circles) and 5% (yellow triangles).

The shorter lifetimes of ExA observed upon degradation have been modelled considering the formation of trapped polarons from diffusing excitons. While we did not observe clear indications of the build-up of a triplet population in the transient experiments, our steady-state PIA clearly indicates the presence of those on a longer time- scale. To explain these observations, we recall that regiorandom P3HT shows signatures of triplets in PIA, while having the same chemical formula of regioregular P3HT.[35] An important difference between the regioregular P3HT used here and regiorandom is the conjugation length and the intrachain planarity, two effects which are known to increase the triplet yield.[47] On the basis of this arguments, we can discuss the increased triplet yield in degraded blends considering that degradation products disrupt the conjugation of the polymer or may create carbonyl groups where intersystem crossing to the triplet manifold is enhanced.[48] The comparison between the losses in DP population and the J_{sc} of solar cells evidences the fact that a large factor in the degradation of photovoltaic performance is ascribed to a shortening of the long timescale recombination (>10 ns), which may also involve charge trapping in PCBM. In this direction, the recent work by Reese et al. reports on the presence of PCBM degradation products acting as effective traps for the transferred electrons.[16]

4. Conclusions

We performed a photophysical study on the fundamental processes enabling photovoltaic action in P3HT/PCBM blends subjected to different ageing periods. The blend films were exposed to a solar simulator in a dry air atmosphere and named according to the relative absorption losses. By combining PL and PIA spectroscopy we can quantify the species affected by degradation, i.e., excitons and polarons. Our analysis of the data, supported by a coupled rate equation model, suggests that exciton trapping can take place on a rate comparable to the one for electron transfer to PCBM. Ageing has major consequences on the polaron generation which is reduced with degradation and has to compete with the fast hot exciton trapping process. The results have important implications for understanding degradation and ageing phenomena in organic solar cells and modelling device losses in aged photovoltaic devices.

5. Experimental Section

Materials: P3HT with a regioregularity of ≥90% was provided by Merck, PC[60]BM was purchased from Solenne and used as received. Thin films of the blends were obtained by doctor-blading on precleaned glass substrates in ambient atmosphere. For all the blends, solutions of the polymer and fullerene were prepared in spectroscopic grade o-xylene. Prior to degradation, the films were annealed at 140 °C in the glovebox for 2 min. Subsequently the samples were degraded by illuminating them with the full spectrum of a sun simulator in dry synthetic air until the desired loss of UV-vis absorption was achieved. Before performing spectroscopy on the degraded samples, they were brought back into the glove box and encapsulated by putting a glass plate on top of the film and sealing the edges with gas-tight epoxy resin (Torrseal). In order to remove any reversibly bound oxygen from the films, the samples were annealed in the glovebox at 130 °C for 10 min before encapsulation.

PL Spectra: were obtained with a double monochromator fluorometer (Jobin-Yvon) equipped with a Peltier and a water cooled detectors sensitive in the NIR spectral range down to 0.8 eV. Measurements were performed exciting at 520 nm by a monochromated Xe lamp, with the sample kept in vacuum at 10^{-6} mbar. No significant differences were observed for samples measured in air, proving the high quality of the encapsulation.

Steady-State PIA: measurements were performed exciting the samples with the second harmonic of a Nd:YAG laser (532 nm) and detecting the laser-induced change in the transmission of a Xenon lamp with a lock-in amplifier. Silicon and InSb detectors were used to cover the visible and near-IR range. The samples were measured under vacuum at room temperature.

Time-Resolved PIA Measurements: Femtosecond transient absorption experiments were performed with a home-built setup starting with a Ti:sapphire regenerative amplifier seeding and optical parametric amplifier. Pulses having a 200 fs duration centred at 550 nm were used as pump, whereas a white light supercontinuum generated in a sapphire plate was used as probe. Detection of the pump-induced changes in the probe beam was performed with a silicon or HgCdTe detectors to cover the visible and near-IR probe beams, referenced to the pump chopping frequency.

Device Preparation and Measurement: For manufacturing the cells, an inverted architecture was chosen, which allows the placement of the electron-blocking layer on top of the photoactive layer. Solar cells in an inverted structure were manufactured in a two-step process as follows. First, after cleaning the glass/ITO substrate by sonication in acetone and isopropanol, an organic hole blocking layer (HBL) was applied, followed by the P3HT:PCBM (ratio 1:0.8) active layer. The obtained half-finished devices were then annealed in a glovebox at 140 °C for 5 min for morphological reasons and degraded in dry synthetic air (80% N_2, 20% O_2, H_2O < 1 ppm) under irradiation of 1 sun afterwards. The progress of degradation was monitored by UV-vis absorption measurement, carried out with a Perkin Elmer UV-VIS Lambda 35 spectrophotometer. After degradation the solar cells were completed in a second step, by applying a highly conductive PEDOT:PSS layer and thermal evaporation of 500 nm of Ag as a metal grid (fingers with a distance of 2 mm and a width of 0.l5 mm). Before evaporation, all devices were annealed in glovebox at 140 °C for 5 min, again, to get only the irreversible degradation of the photoactive layer. All layers are applied out of solution by doctor blading.

For characterization, the cells were illuminated with the AM1.5 g spectrum of a Steuernagel Solartest 1200 solar simulator at 100 mW cm^{-2}. *J–V* characteristics (current density vs. voltage) were recorded using a Keithley 2400 SMU together with a Keithley 7001 Multiplexer system and custom software. The degradation was done in glovebox to avoid further degradation.

Acknowledgements

The authors thank S. Niedermaier and A. Helfrich for technical assistance. The authors are grateful to the DFG for financial support through the SPP1355 "Fundamental processes in Organic photovoltaics" and the BMBF through "OPVstabil" and "EOS". The German Excellence Initiative is also acknowledged for funding via the "Nanosystems Initiative Munich (NIM)".

Received: August 16, 2011
Revised: October 10, 2011
Published online: January 30, 2012

[1] G. Dennler, M. C. Scharber, C. J. Brabec, *Adv. Mater.* **2009**, *21*, 1323.
[2] J. Y. Kim, K. Lee, N. E. Coates, D. Moses, T. Q. Nguyen, M. Dante, A. J. Heeger, *Science* **2007**, *317*, 222.
[3] M. A. Green, K. Emery, Y. Hishikawa, W. Warta, *Prog. Photovoltaics* **2011**, *19*, 84.

[4] H. Y. Chen, J. H. Hou, S. Q. Zhang, Y. Y. Liang, G. W. Yang, Y. Yang, L. P. Yu, Y. Wu, G. Li, *Nat. Photonics* **2009**, *3*, 649.
[5] R. Gaudiana, C. Brabec, *Nat. Photonics* **2008**, *2*, 287.
[6] M. Jorgensen, K. Norrman, F. C. Krebs, *Sol. Energy Mater. Sol. Cells* **2008**, *92*, 686.
[7] A. Kumar, R. Devine, C. Mayberry, B. Lei, G. Li, Y. Yang, *Adv. Funct. Mater.* **2010**, *20*, 2729.
[8] R. Lessmann, Z. Hong, S. Scholz, B. Maennig, M. K. Riede, K. Leo, *Org. Electron.* **2010**, *11*, 539.
[9] C. Lin, E. Y. Lin, F. Y. Tsai, *Adv. Funct. Mater.* **2010**, *20*, 834.
[10] M. O. Reese, A. J. Morfa, M. S. White, N. Kopidakis, S. E. Shaheen, G. Rumbles, D. S. Ginley, *Sol. Energy Mater. Sol. Cells* **2008**, *92*, 746.
[11] T. Tromholt, E. A. Katz, B. Hirsch, A. Vossier, F. C. Krebs, *Appl. Phys. Lett.* **2010**, *96*, 073501.
[12] R. Steim, S. A. Choulis, P. Schilinsky, U. Lemmer, C. J. Brabec, *Appl. Phys. Lett.* **2009**, *94*, 043304.
[13] B. Ecker, J. C. Nolasco, J. Pallarés, L. F. Marsal, J. Posdorfer, J. Parisi, E. von Hauff, *Adv. Funct. Mater.* **2011**, *21*, 2705.
[14] A. Seemann, T. Sauermann, C. Lungenschmied, O. Armbruster, S. Bauer, H.-J. Egelhaaf, J. Hauch, *Sol. Energy* **2011**, *85*, 1238.
[15] M. S. M. Seeland, R. Rosch, H. Hoppe, *J. Appl. Phys.* **2011**, *109*, 064513.
[16] M. O. Reese, A. M. Nardes, B. L. Rupert, R. E. Larson, D. C. Olson, M. T. Lloyd, S. E. Shaheen, D. S. Ginley, G. Rumbles, N. Kopidakis, *Adv. Funct. Mater.* **2010**, *20*, 3476.
[17] G. Dicker, M. P. de Haas, L. D. A. Siebbeles, J. M. Warman, *Phys. Rev. B* **2004**, *70*, 045203.
[18] S. Cook, H. Ohkita, Y. Kim, J. J. Benson-Smith, D. D. C. Bradley, J. R. Durrant, *Chem. Phys. Lett.* **2007**, *445*, 276.
[19] W. Guss, J. Feldmann, E. O. Göbel, C. Taliani, H. Mohn, W. Muller, P. Haussler, H. U. Termeer, *Phys. Rev. Lett.* **1994**, *72*, 2644.
[20] H. Schlaich, M. Muccini, J. Feldmann, H. Bässler, E. O. Göbel, R. Zamboni, C. Taliani, J. Erxmeyer, A. Weidinger, *Chem. Phys. Lett.* **1995**, *236*, 135.
[21] J. Piris, T. E. Dykstra, A. A. Bakulin, P. H. M. van Loosdrecht, W. Knulst, M. T. Trinh, J. M. Schins, L. D. A. Siebbeles, *J. Phys. Chem. C* **2009**, *113*, 14500.
[22] C. X. Sheng, M. Tong, S. Singh, Z. V. Vardeny, *Phys. Rev. B* **2007**, *75*, 085206.
[23] X. M. He, F. Gao, G. L. Tu, D. Hasko, S. Huttner, U. Steiner, N. C. Greenham, R. H. Friend, W. T. S. Huck, *Nano Lett.* **2010**, *10*, 1302.
[24] M. Schubert, C. H. Yin, M. Castellani, S. Bange, T. L. Tam, A. Sellinger, H. H. Horhold, T. Kietzke, D. Neher, *J. Chem. Phys.* **2009**, *130*, 094703.
[25] G. Yu, J. Gao, J. C. Hummelen, F. Wudl, A. J. Heeger, *Science* **1995**, *270*, 1789.
[26] M. Hallermann, E. Da Como, J. Feldmann, M. Izquierdo, S. Filippone, N. Martin, S. Juchter, E. von Hauff, *Appl. Phys. Lett.* **2010**, *97*, 023301.
[27] M. Hallermann, I. Kriegel, E. Da Como, J. M. Berger, E. von Hauff, J. Feldmann, *Adv. Funct. Mater.* **2009**, *19*, 3662.
[28] D. Veldman, O. Ipek, S. C. J. Meskers, J. Sweelssen, M. M. Koetse, S. C. Veenstra, J. M. Kroon, S. S. van Bavel, J. Loos, R. A. J. Janssen, *J. Am. Chem. Soc.* **2008**, *130*, 7721.
[29] T. M. Clarke, J. R. Durrant, *Chem. Rev.* **2010**, *110*, 6736.
[30] J. Schafferhans, A. Baumann, C. Deibel, V. Dyakonov, *Appl. Phys. Lett.* **2008**, *93*, 1693.
[31] P. W. M. Blom, V. D. Mihailetchi, L. J. A. Koster, D. E. Markov, *Adv. Mater.* **2007**, *19*, 1551.
[32] Y. Kim, S. Cook, S. M. Tuladhar, S. A. Choulis, J. Nelson, J. R. Durrant, D. D. C. Bradley, M. Giles, I. McCulloch, C. S. Ha, M. Ree, *Nat. Mater.* **2006**, *5*, 197.
[33] J. R. Lakowicz, *Principles of Fluorescence Spectroscopy*, Springer, Singapore **1999**.
[34] H. Hintz, H. Peisert, H. J. Egelhaaf, T. Chassé, *J. Phys. Chem. C* **2011**, *115*, 13373.
[35] R. Österbacka, C. P. An, X. M. Jiang, Z. V. Vardeny, *Science* **2000**, *287*, 839.
[36] H. Sirringhaus, P. J. Brown, R. H. Friend, M. M. Nielsen, K. Bechgaard, B. M. W. Langeveld-Voss, A. J. H. Spiering, R. A. J. Janssen, E. W. Meijer, P. Herwig, D. M. de Leeuw, *Nature* **1999**, *401*, 685.
[37] J. Guo, H. Ohkita, S. Yokoya, H. Benten, S. Ito, *J. Am. Chem. Soc.* **2010**, *132*, 9631.
[38] J. M. Guo, H. Ohkita, H. Benten, S. Ito, *J. Am. Chem. Soc.* **2010**, *132*, 6154.
[39] X. M. Jiang, R. Österbacka, O. Korovyanko, C. P. An, B. Horovitz, R. A. J. Janssen, Z. V. Vardeny, *Adv. Funct. Mater.* **2002**, *12*, 587.
[40] G. Hukic-Markosian, Z. V. Vardeny, *Synth. Met.* **2010**, *160*, 314.
[41] J. M. Hodgkiss, A. R. Campbell, R. A. Marsh, A. Rao, S. Albert-Seifried, R. H. Friend, *Phys. Rev. Lett.* **2010**, *104*, 177701.
[42] I. W. Hwang, D. Moses, A. J. Heeger, *J. Phys. Chem. C* **2008**, *112*, 4350.
[43] T. Drori, J. Holt, Z. V. Vardeny, *Phys. Rev. B* **2010**, *82*, 075207.
[44] R. Kersting, U. Lemmer, R. F. Mahrt, K. Leo, H. Kurz, H. Bässler, E. O. Göbel, *Phys. Rev. Lett.* **1993**, *70*, 3820.
[45] R. A. Marsh, J. M. Hodgkiss, R. H. Friend, *Adv. Mater.* **2010**, *22*, 3672.
[46] E. Collini, G. D. Scholes, *Science* **2009**, *323*, 369.
[47] D. Beljonne, Z. Shuai, G. Pourtois, J. L. Brédas, *J. Phys. Chem. A* **2001**, *105*, 3899.
[48] N. Turro, *Modern Molecular Photochemistry*, University Science Books, Palo Alto, CA **1991**.